Shades of red and green : the colorful diversity and ecology of picocyanobacteria in the Baltic Sea

Haverkamp, T.H.A.

Chapter 2

Colourful coexistence of red and green picocyanobacteria in lakes and seas

Maayke Stomp[1]
Jef Huisman[1*]
Lajos Vörös[2]
Frances R. Pick[3]
Maria Laamanen[4]
Thomas Haverkamp[5]
Lucas J. Stal[5]

[1]*Aquatic Microbiology, Institute for Biodiversity and Ecosystem Dynamics, University of Amsterdam, Nieuwe Achtergracht 127, 1018 WS Amsterdam, The Netherlands*
[2]*Balaton Limnological Research Institute of the Hungarian Academy of Sciences, PO Box 35, H-8237 Tihany, Hungary*
[3]*Biology Department, University of Ottawa, PO Box 450, Ottawa, ON K1N 6N5, Canada*
[4]*Finnish Institute of Marine Research, PO Box 2, FIN-00561 Helsinki, Finland (Present address: Ministry of the Environment, PO Box 35, FIN-00023 Government, Finland)*
[5]*Netherlands Institute of Ecology (NIOO-KNAW), Centre for Estuarine and Marine Ecology, PO Box 140, 4400 AC Yerseke, The Netherlands*

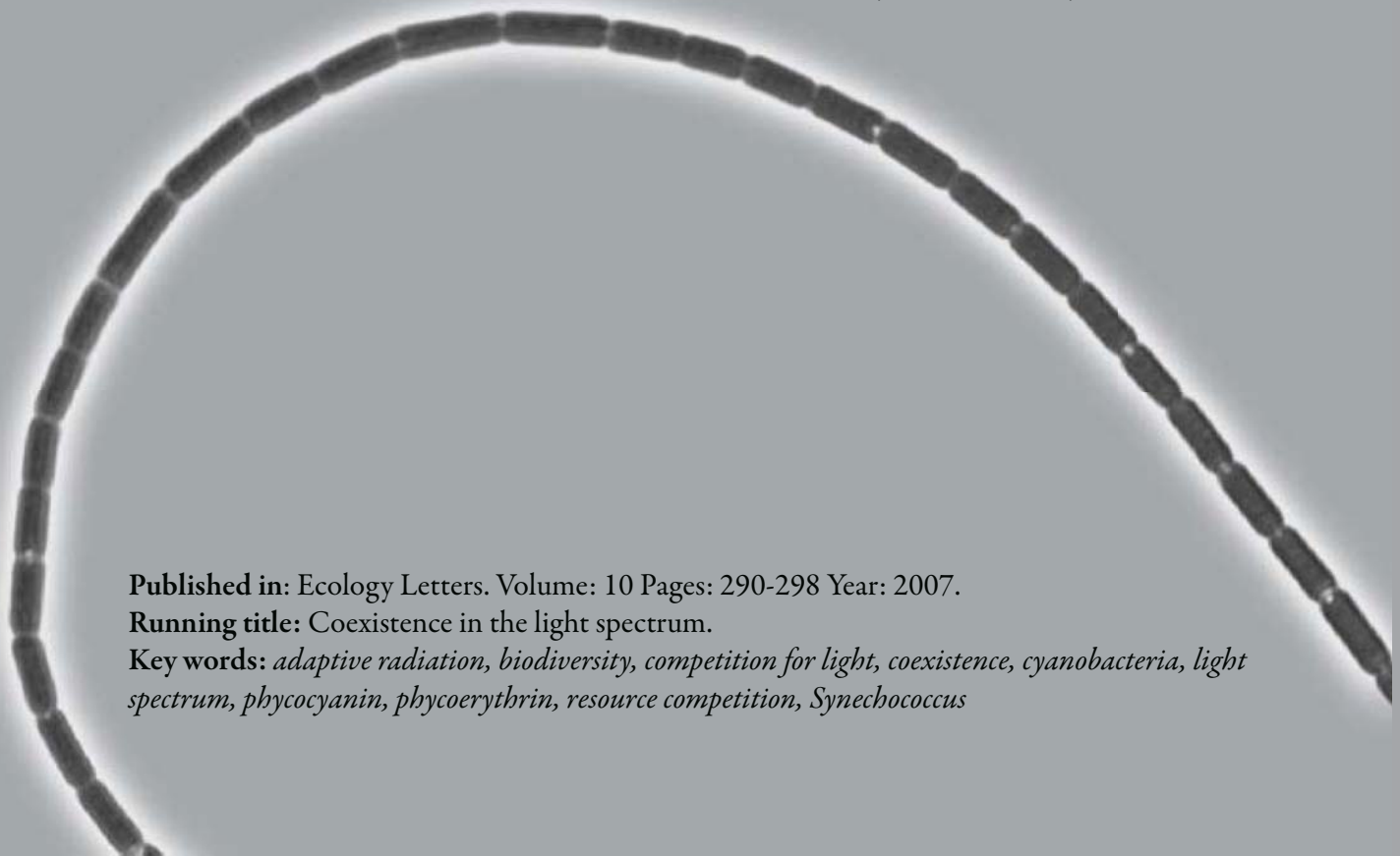

Published in: Ecology Letters. Volume: 10 Pages: 290-298 Year: 2007.
Running title: Coexistence in the light spectrum.
Key words: *adaptive radiation, biodiversity, competition for light, coexistence, cyanobacteria, light spectrum, phycocyanin, phycoerythrin, resource competition, Synechococcus*

Abstract

The paradox of the plankton inspired many studies on the mechanisms of species coexistence. Recent laboratory experiments showed that partitioning of white light allows stable coexistence of red and green picocyanobacteria. Here, we investigate to what extent these laboratory findings can be extrapolated to natural waters. We predict from a parameterised competition model that the underwater light colour of lakes and seas provides ample opportunities for coexistence of red and green phytoplankton species. To test this prediction, we sampled picocyanobacteria of 70 aquatic ecosystems, ranging from clear blue oceans to turbid brown peat lakes. As predicted, red picocyanobacteria dominated in clear waters whereas green picocyanobacteria dominated in turbid waters. We found widespread coexistence of red and green picocyanobacteria in waters of intermediate turbidity. These field data support the hypothesis that niche differentiation along the light spectrum promotes phytoplankton biodiversity, thus providing a colourful solution to Hutchinson's plankton paradox.

Introduction

Phytoplankton species compete for only a handful of resources (e.g., nitrogen, phosphorus, iron, silica, light). This suggests limited opportunity for niche differentiation. Yet, a single millilitre of water may contain dozens of different phytoplankton species. What explains the surprising biodiversity of the plankton? This paradox of the plankton, formulated by Hutchinson (1961), has motivated a plethora of studies on competition and community structure (Tilman 1982; Sommer 1985; Grover 1997; Huisman & Weissing 1999; Litchman & Klausmeier 2001). Classic ecological theory predicts that niche differentiation reduces competition among species, and thereby facilitates coexistence (Gause 1934; MacArthur & Levins 1967; Hutchinson 1978). Darwin's finches are a famous example (Darwin 1859; Lack 1974). A rich variety of finch species coexist on the Galápagos islands, as adaptive radiation in beak morphology has enabled niche differentiation of the finch species along a spectrum of different seed sizes (Grant & Grant 2002).

Similarly, light offers a spectrum of resources, ranging from blue light at short wavelengths, via green and yellow, to red light at long wavelengths. Although competition theory has largely ignored the light spectrum as a major axis of niche differentiation, plankton ecologists have long recognized that a rich diversity of photosynthetic pigments allows phytoplankton species to utilize different wavelengths (Engelmann 1883; Bricaud *et al*. 1983; Wood 1985; Sathyendranath & Platt 1989; Kirk 1994; Falkowski *et al*. 2004). For instance, red picocyanobacteria use the pigment phycoerythrin to absorb green light, whereas green picocyanobacteria use the pigment phycocyanin to absorb red light (Fig. 2.1a). Hence, one might hypothesize that they can share the light spectrum by specialization on different wavelengths. Indeed, recent competition models and laboratory experiments showed that red picocyanobacteria win the competition in green light, green picocyanobacteria win in red light, while red and green picocyanobacteria coexist in the full spectrum provided by white light (Stomp *et al*. 2004). One might argue, however, that underwater light fields do not resemble a white spectrum, because water, dissolved organic matter, and other constituents bring colour into the water column. Can these models and laboratory experiments be extrapolated to natural waters? Does partitioning of the underwater light spectrum mediate the coexistence of a colourful mixture of phytoplankton species in aquatic ecosystems?

To address these questions, we apply a fully parameterised competition model to predict the outcome of competition between red and green phytoplankton species in different natural waters. We test the model predictions by sampling red and green picocyanobacteria from many different aquatic ecosystems, ranging from clear blue oceans to dark brown peat lakes.

Competition model

The underwater light spectrum of natural waters largely depends on light attenuation by water itself, by the "background turbidity" caused by dissolved organic matter (known as gilvin in the optics literature) and inanimate suspended particles (tripton, like sediment and detritus), and by the phytoplankton species present in the water column (Kirk 1994). Water absorbs

strongly in the red part of the spectrum, whereas the background turbidity is responsible for rapid attenuation of blue wavelengths (Fig. 2.1b). Hence, with increasing background turbidity, the underwater light spectrum is shifted towards the red. The total light absorption by all these constituents determines the underwater light spectrum. For example, in the Baltic Sea light absorption in the blue and the red end of the spectrum is of a similar magnitude (Fig. 2.1b), resulting in an underwater light spectrum that narrows to the green wavelengths (Fig. 2.1c).

We consider a vertical water column, in which the phytoplankton species, gilvin and tripton are all homogeneously mixed throughout the surface mixed layer. Let I(λ,*z*) denote the light intensity of wavelength λ at depth z. Sunlight enters the water column with an incident light spectrum Iin(λ). According to a spectrally explicit version of Lambert-Beer's law, the underwater light spectrum changes with depth (Sathyendranath & Platt 1989; Kirk 1994; Stomp et al. 2004):

$$(\lambda, z) = I_{in}(\lambda) EXP\left(-K_W(\lambda)z - K_{BG}(\lambda)z - \sum_{i=1}^{n} k_i(\lambda)N_i z\right) \qquad (1)$$

where KW(λ) is the absorption spectrum of water, KBG(λ) is the absorption spectrum of the background turbidity (tripton plus gilvin), ki(λ) is the specific absorption spectrum of phytoplankton species i, Ni is the population density of phytoplankton species i, and n is the number of phytoplankton species. We note, from Eq.1, that the underwater light spectrum is dynamic. For instance, changes in the population densities of phytoplankton species can shift the underwater light spectrum.

The number of absorbed photons available for photosynthesis by a phytoplankton species *i* at a given depth *z* depends on its photosynthetic action spectrum and on the light spectrum at this depth (Sathyendranath & Platt 1989; Stomp *et al*. 2004):

$$\gamma_i(z) = \int_{400}^{700} a_i(\lambda)k_i(\lambda)I(\lambda, z)d\lambda \qquad (2)$$

where $a_i(\lambda)$ converts the absorption spectrum into the action spectrum of phytoplankton species *i*. In many species, photons that have been absorbed are utilized with equal efficiency, irrespective of their wavelengths. That is, the absorption spectrum and action spectrum are often quite similar (Kirk 1994; Lewis *et al*. 1985). For simplicity, therefore, we here assume that the absorption spectrum and action spectrum have the same shape (i.e., $a_i(\lambda) = 1$ for all λ). We further assume that the specific growth rate of each phytoplankton species *i* is an increasing, saturating function of the number of photons it has absorbed (Sathyendranath & Platt 1989):

$$\frac{dN_i}{dt} = \frac{N_i}{z_m}\int_0^{z_m} \frac{p_{max,i}\gamma_i(z)}{(p_{max,i}/\phi_i) + \gamma_i(z)}dz - L_i N_i \qquad i = 1, ..., n \qquad (3)$$

where $p_{\max,i}$ is the maximum specific growth rate of species *i*, ϕ_i is the growth efficiency ('quantum yield') at low light intensities, L_i is the specific loss rate due to factors such as grazing

and sinking, and z_m is the depth of the surface mixed layer. Essentially, Eq.3 states that the growth rates of the species are governed by the photons they have absorbed. That is, there is no direct interference between the species. Instead, the species compete for light by absorption of photons in specific regions of the light spectrum. Species with similar light absorption spectra will therefore face stronger competition for light.

Numerical simulations of the model were based on a fourth order Runga-Kutta procedure for time integration, and Simpson's rule for depth integration. Model parameters for our simulations were obtained as follows. For the incident light spectrum, $I_{in}(\lambda)$, we used the

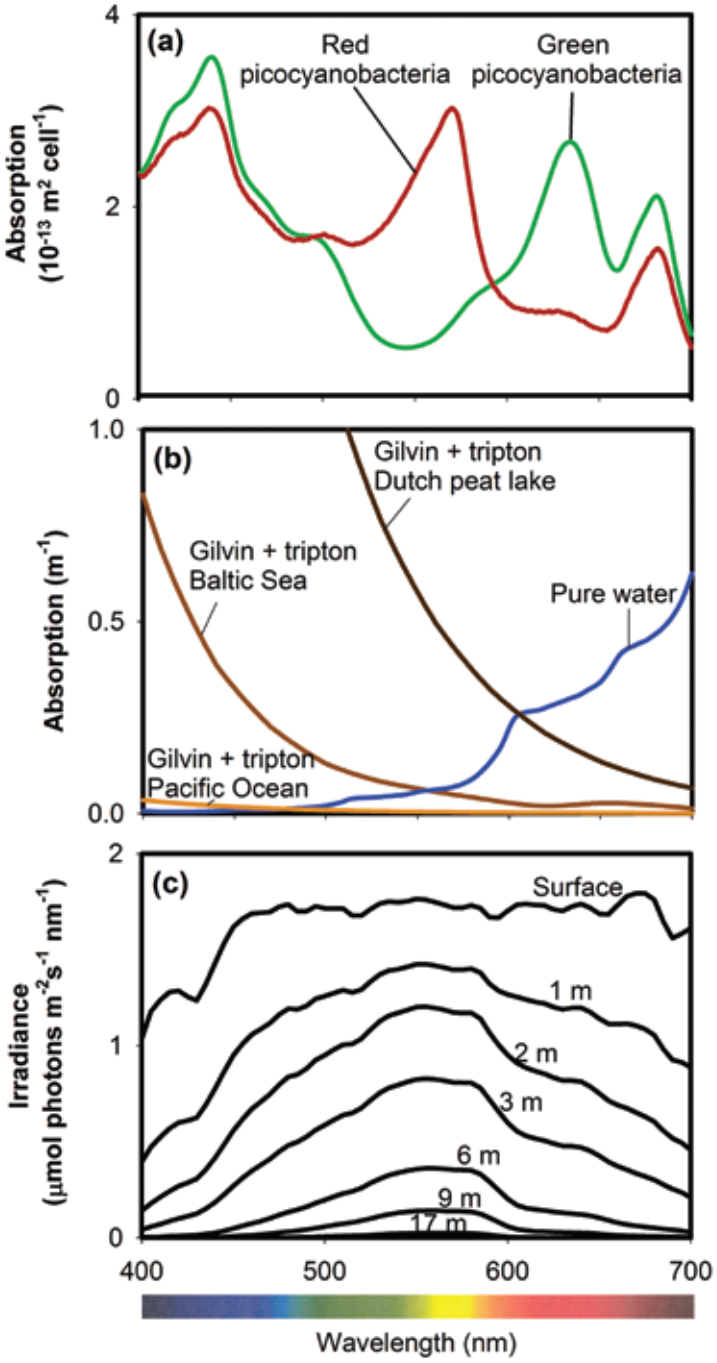

Figure 2.1 *Optical characteristics of red and green picocyanobacteria and their environment. (a) Absorption spectra of red and green picocyanobacteria isolated from the Baltic Sea. (b) Light absorption spectra of pure water (blue line) and gilvin plus tripton in the Pacific Ocean (light brown line), the Baltic Sea (medium brown), and a peat lake (dark brown). (c) Underwater light spectra measured in the Baltic Sea. The spectrum narrows to the green waveband with increasing depth.*

surface spectrum measured at the Baltic Sea on July 2004 (Fig. 2.1c). The absorption spectrum of pure water was taken from the literature (Pope & Fry 1997). The absorption spectrum of the background turbidity can be described as an exponentially decreasing function of wavelength (Bricaud *et al.* 1981; Kirk 1994):

$$K_{BG}(\lambda) = K_{BG}(484)EXP(-S(\lambda - 484)) \qquad (4)$$

where $K_{BG}(484)$ is the background turbidity at a reference wavelength of 484 nm, and S is the slope of the exponential decline. The value of $K_{BG}(484)$ depends on the concentration of gilvin and tripton (see Supplementary Material). The slope S varies between 0.010 and 0.020 nm^{-1}, and we will here assume a typical value of S = 0.017 nm^{-1} (Kirk 1994). The growth and loss parameters of the picocyanobacteria (p_{max}, ϕ, L) were estimated from our earlier studies (Lavallée & Pick 2002; Stomp *et al.* 2004). We assumed that the parameter values of red and green picocyanobacteria are identical, except for their absorption spectra. The specific absorption spectra of red and green picocyanobacteria were measured with an AMINCO DW-2000 double-beam spectrophotometer (Stomp *et al.* 2004), and are shown in Fig. 2.1a. Parameter values and their sources are listed in Table 2.1.

Table 2.1 *Parameter values and their interpretation*

Symbol	Interpretation	Units	Value
Independent variables			
t	time	d	-
z	depth	m	-
λ	wavelength	nm	-
Dependent variables			
N_i	Population density of species i	cells m^{-3}	-
$\gamma_i(z)$	Absorbed photons by species i	µmol photons $cell^{-1}$ s^{-1}	-
$I(\lambda, z)$	Underwater light spectrum	µmol photons m^{-2} s^{-1} nm^{-1}	-
Parameters			
$I_{in}(\lambda)$	Spectrum of incident light	µmol photons m^{-2} s^{-1} nm^{-1}	Measured (Fig.1c)
$K_W(\lambda)$	Absorption spectrum of pure water	m^{-1}	Literature*
$K_{BG}(\lambda)$	Absorption spectrum of background turbidity (tripton plus gilvin)	m^{-1}	Calculated (Eq.2)
$K_{BG}(484)$	Absorption of background turbidity at 484 nm	m^{-1}	Measured range (0.03 – 7.0)
S	Exponential decline of absorption spectrum of background turbidity	nm^{-1}	0.017†
$k_i(\lambda)$	Absorption spectrum of species i	m^2 $cell^{-1}$	Measured (Fig.1a)
$a_i(\lambda)$	Conversion of absorption spectrum into action spectrum of species i	-	1
z_m	Depth of surface mixed layer	m	Wide range (1 – 100)
L_i	Specific loss rate of species i	d^{-1}	0.67‡
$p_{max,i}$	Maximum growth rate of species i	d^{-1}	1.0‡
φ_i	Photosynthetic efficiency of species i	cells d^{-1} (µmol photons $s^{-1})^{-1}$	2.0 x 10^{12} §

*Notes: *Pope & Fry (1997); †Kirk (1994); ‡Lavallée & Pick (2002); §Stomp et al. (2004).*

Materials and Methods

Sampling picocyanobacteria.

We sampled picocyanobacteria from a wide variety of waters covering a large range of background turbidities. Our sampling sites included station ALOHA in the subtropical Pacific Ocean, 9 sampling stations in the Baltic Sea, and 60 lakes in Canada, Hungary, Italy, Nepal and New Zealand. An overview of all 70 sampling stations is given in the Supplementary Material.

Counting picocyanobacteria.

The concentrations of red and green picocyanobacteria in samples from the Baltic Sea and Pacific Ocean were counted by flow cytometry (Jonker *et al.* 1995; Vives-Rego *et al.* 2000), using a Coulter Epics Elite ESP flow cytometer (Beckman Coulter Nederland BV, Mijdrecht, Netherlands) equipped with a green laser (525 nm) and a red laser (670 nm). The flow cytometer distinguished between picocyanobacteria and larger phytoplankton by their size (using side scattering). Red and green picocyanobacteria were distinguished based upon their different fluorescence signals. Cells rich in phycoerythrin emitted orange light (550-620 nm) when excited by the green laser, whereas cells rich in phycocyanin emitted far red light (> 670 nm) when excited by the red laser.

The concentrations of red and green picocyanobacteria in the lake samples were counted by epifluorescence microscopy using blue and green filters (Pick 1991; Vörös *et al.* 1998). When excited by blue light, cells rich in phycoerythrin emit yellow to orange light, while cells without phycoerythrin appear dull red. When excited by green light, both red and green picocyanobacteria emit an intense red light. Both groups of picocyanobacteria can be easily distinguished from eukaryotic picoplankton or prochlorophytes, which fluoresce a very faint red or not at all.

Light spectra and absorption spectra.

Spectra of the incident light and underwater light spectra were measured with a RAMSES-ACC-VIS spectroradiometer (TriOS, Oldenburg, Germany). Absorption spectra of background turbidity were calculated by Eq.2, from the light attenuation of background turbidity at the reference wavelength of 484 nm, $K_{BG}(484)$. Further methodological details can be found in the Supplementary Material.

Results

Model Predictions

We used the model to simulate competition for light between red and green picocyanobacteria in different underwater light fields. As a first check, we ran a large number of simulations to investigate the model's behaviour. The model did not display non-equilibrium dynamics or multiple stable states. Each simulation was run until changes in population densities approached zero, and hence an equilibrium had been reached. In all simulations, the final outcome of competition was always independent of the initial abundances of the species.

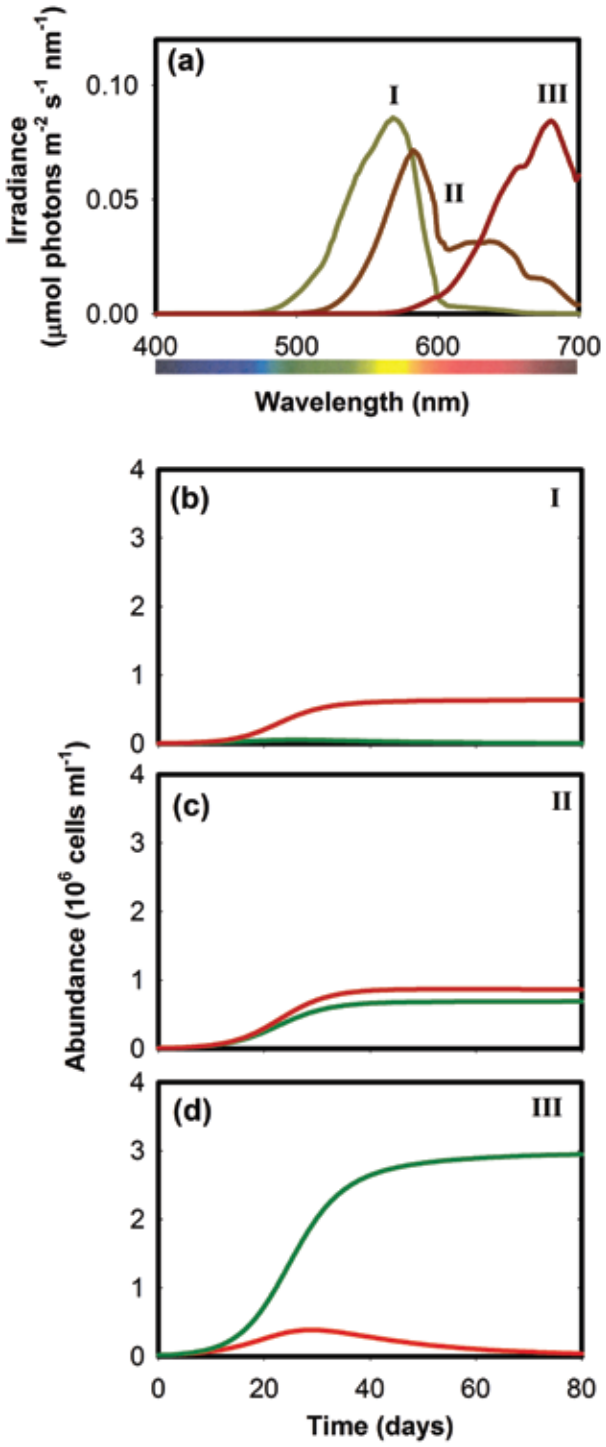

Fig. 2.2a shows the underwater light spectra at the photic depth (defined as the depth at which the PAR-integrated irradiance equals 1% of the surface irradiance), calculated from Eqs.1 and 2, for three waters with different background turbidities. When background turbidity is low, typical of oligotrophic lakes, the underwater light spectrum is green (Fig. 2.2a), which matches the absorption spectrum of red picocyanobacteria (Fig. 2.1a). In this environment, the model predicts that red picocyanobacteria win (Fig. 2.2b). At intermediate background

Figure 2.2 *Model simulations. (a) Light spectra at the photic depth in waters with, I, a low background turbidity ($K_{BG}(484)$ = 0.3 m^{-1}), II, intermediate background turbidity ($K_{BG}(484)$ = 1.1 m^{-1}), and III, high background turbidity ($K_{BG}(484)$ = 7 m^{-1}). (b) Red picocyanobacteria win in clear waters with a deep surface-mixed layer ($K_{BG}(484)$=0.3 m^{-1}; z_m=36 m). (c) Stable coexistence of red and green picocyanobacteria in waters of intermediate turbidity and mixing depth ($K_{BG}(484)$=1.1 m^{-1}; z_m=17 m). (d) Green picocyanobacteria win in turbid waters with a shallow surface-mixed layer ($K_{BG}(484)$=7 m^{-1}; z_m=8 m).*

turbidity typical for mesotrophic lakes and the coastal zone, the underwater light spectrum (Fig. 2.2a) overlaps with the absorption spectra of both picocyanobacteria. Here, the model predicts stable coexistence of red and green picocyanobacteria (Fig. 2.2c). At high background turbidity, typical of eutrophic lakes, the underwater light spectrum is shifted towards the red (Fig. 2.2a), and here green picocyanobacteria are the superior competitors (Fig. 2.2d). Thus, along a gradient of background turbidity, theory predicts that red picocyanobacteria are gradually replaced by green picocyanobacteria.

Fig. 2.3 plots the outcome of competition as a function of background turbidity and mixing depth of the surface mixed layer. If the surface mixed layer is deep and the background turbidity is high (upper right area in Fig. 2.3), conditions are too dark for the growth of picocyanobacteria. If the surface mixed layer is shallow (lower part of Fig. 2.3), the picocyanobacteria are exposed to the white light spectrum near the water surface, in which both the red and green species can coexist. If the surface mixed layer has an intermediate depth, the model predicts a gradual transition from red to green picocyanobacteria with increasing background turbidity (Fig. 2.3).

Testing the Model Predictions in Lakes and Seas

We first tested the model predictions in the Baltic Sea. Here, we found widespread coexistence of red and green picocyanobacteria. At sampling stations with a deep surface mixed layer, the reds and greens typically coexisted throughout

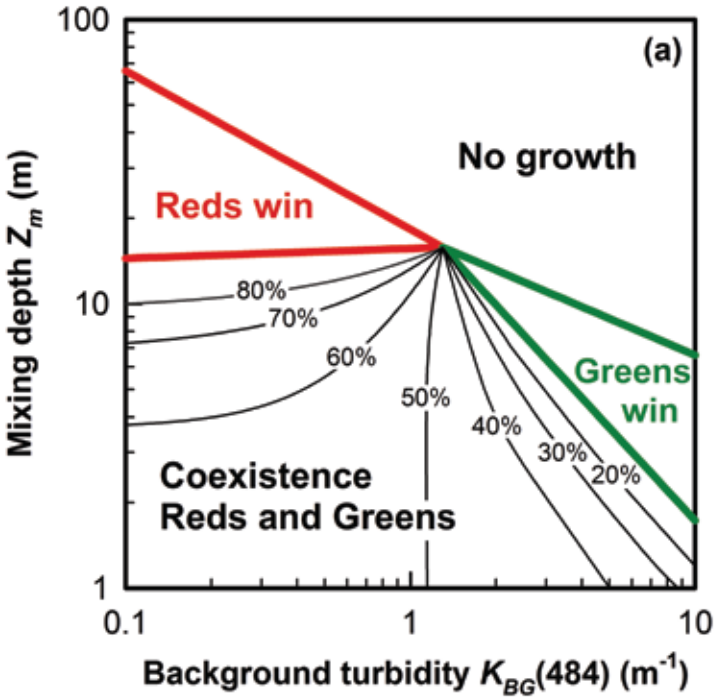

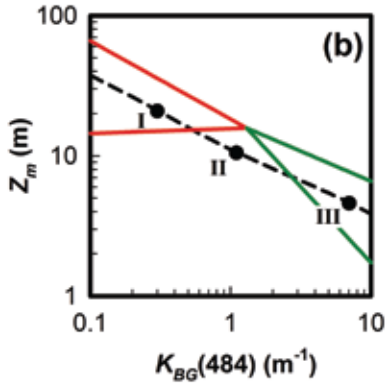

Figure 2.3 *The predicted outcome of competition plotted as function of background turbidity and surface-mixed-layer depth. The graph is based on a grid of 100 x 100 simulations. Dashed line indicates the photic depth, which depends on the background turbidity of the water column. Points I, II, and III correspond to the simulations shown in Figure 2.2. Model parameters: see Table 2.1.*

the surface layer (Fig. 2.4a). At sampling stations with a shallower surface mixed layer, the red and green picocyanobacteria coexisted near the surface while red picocyanobacteria formed a deep chlorophyll maximum underneath (Fig. 2.4b). Isolation of picoplankton strains from the Baltic Sea revealed a colourful community of picocyanobacteria and pico-eukaryotes (Fig. 2.4c), spanning a full rainbow from red to green pigmentation. Analysis of the sequences of the 16S rRNA gene and the ribosomal internally transcribed spacer (ITS-1) region show that the varicoloured picocyanobacteria of the Baltic Sea are all closely related and fall within the subalpine cluster II and the Bornholm Sea cluster of the *Synechococcus* complex (Crosbie *et al*. 2003; Ernst *et al*. 2003). Fig. 2.4c thus illustrates that closely related picocyanobacteria may radiate into a rich variety of differently pigmented strains.

As a next step, we extended the analysis to the complete data set of 70 sampling stations, covering a wide range of background turbidities (see Table S1 of the Supplementary Materials for details). At low background turbidity ($K_{BG}(484) < 0.6\ m^{-1}$), red picocyanobacteria were dominant (Fig. 2.5). At high background turbidity ($K_{BG}(484) > 3\ m^{-1}$), green picocyanobacteria were dominant. The data set shows coexistence of reds and greens in a large window of intermediate background turbidities. For comparison, model predictions are plotted by the

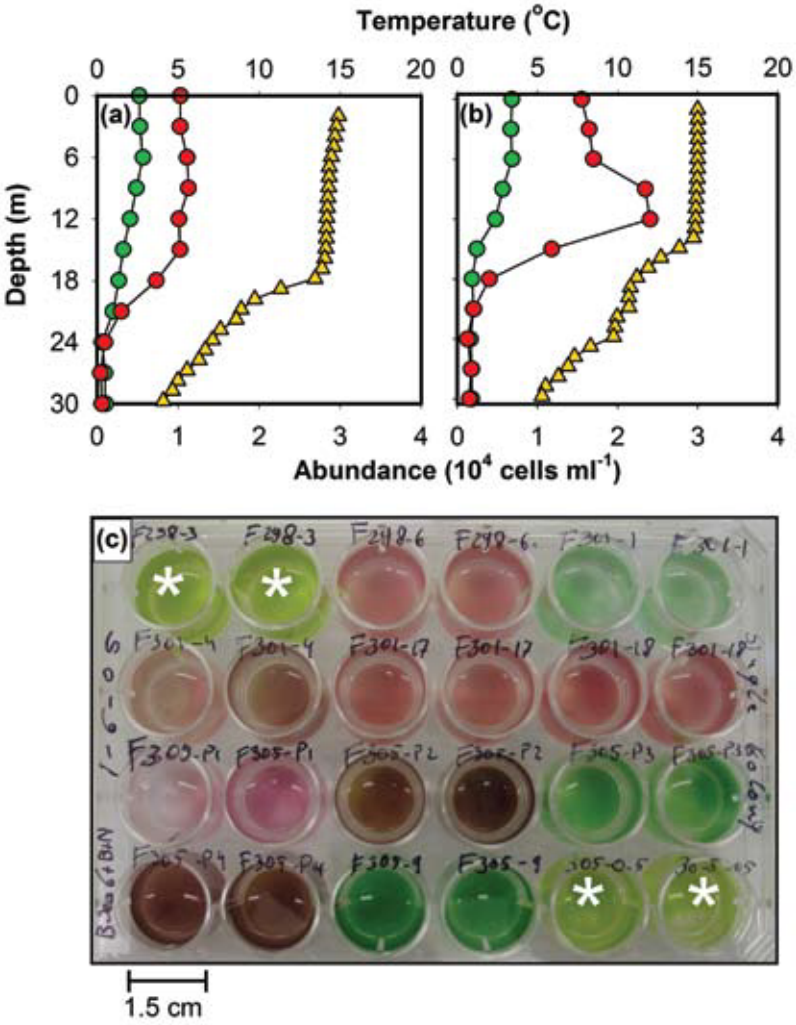

Figure 2.4 *Coexistence of red and green picocyanobacteria in the Baltic Sea. (a) Depth profiles from a sampling station with a homogeneous distribution of coexisting red and green picocyanobacteria up to a depth of 18 m. (b) Depth profiles from a sampling station with a homogeneous distribution of coexisting reds and greens near the surface, and a deep chlorophyll maximum of red picocyanobacteria underneath. Red circles indicate red picocyanobacteria, green circles indicate green picocyanobacteria, yellow triangles indicate temperature. (c) Picoplankton strains isolated from the Baltic Sea, illustrating a colourful biodiversity of green pico-eukaryotes (the wells indicated by a *) and varicoloured picocyanobacteria of the subalpine cluster II of* Synechococcus *(all other wells).*

solid lines in Fig. 2.5, assuming that the surface-mixed-layer depth equals the photic depth, which corresponds to a slice along the dashed line in Fig. 2.3. The competition model predicts a similar transition from red to green picocyanobacteria as observed in the sampled lakes and seas. Linear regression of predicted versus observed relative abundances revealed that the model explained 54% of the variation in the data set ($R^2 = 0.54$, $n = 70$, $P < 0.0001$). Linear regression of the residuals versus background turbidity was not significant ($R^2 = 0.01$, $n = 70$, P = 0.20). This indicates that the model effectively captured the relationship between the relative abundances of red and green picocyanobacteria and background turbidity.

As a final check, we tested the sensitivity of the model predictions to our simplifying assumption that the surface-mixed-layer depth equaled the photic depth (where irradiance is 1% of surface irradiance). For this purpose, we ran the model using a shallower and a deeper surface mixed layer, corresponding to 0.5% and 5% of the surface irradiance, respectively. This showed that the model predictions were not very sensitive to our assumption. The coexistence window in Fig. 2.5 slightly widened or narrowed, respectively, and the model still explained 43% to 33% of the variation in the data set.

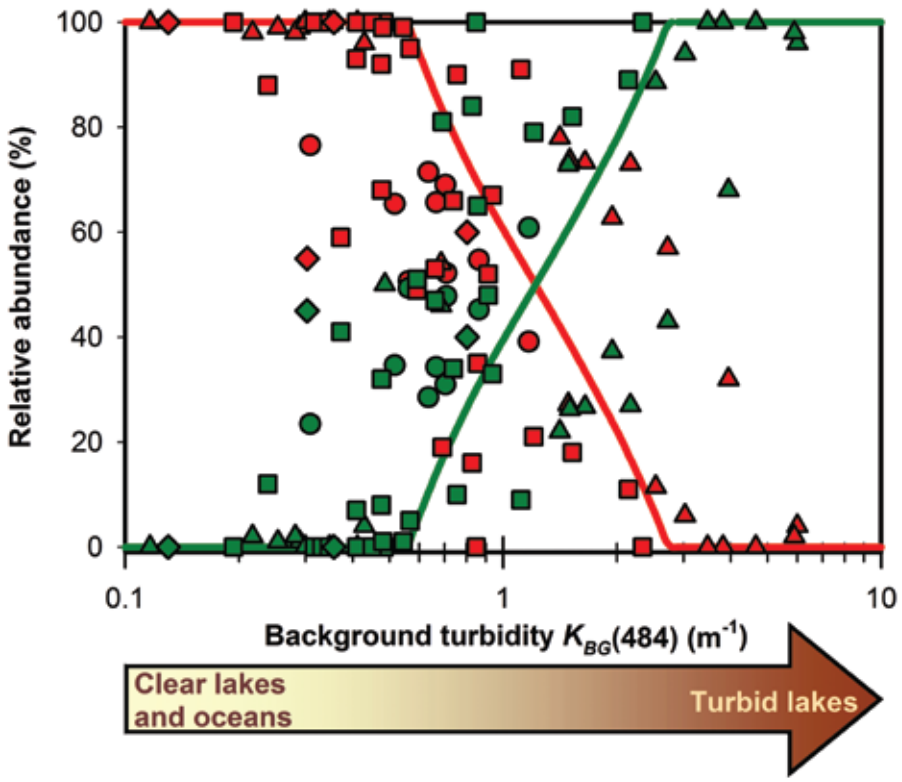

Figure 2.5 *Relative abundances of red picocyanobacteria (red symbols) and green picocyanobacteria (green symbols) observed in lakes and seas plotted against background turbidity. Data are from 25 European lakes (triangles), 30 Canadian lakes (squares), 5 lakes in Nepal and New Zealand (diamonds), and 9 sampling stations in the Baltic Sea (circles). At sampling station ALOHA, in the subtropical Pacific, background turbidity was below the range shown in the graph, but the picocyanobacteria of the* Synechococcus *group were dominated by nearly 100% red cells. The red and green curves indicate the model predictions for red and green picocyanobacteria, respectively, assuming a surface-mixed-layer depth equal to the photic depth. Model parameters: see Table 2.1.*

Discussion

Many previous studies have focused on light intensity as a major axis of niche differentiation in aquatic and terrestrial plant communities. Theory and experiments have shown that competition for light can be successfully predicted from knowledge of species traits and environmental conditions (Huisman *et al*. 1999; Litchman 2003; Passarge *et al*. 2006). Field studies have shown that light intensity is an important selective factor in phytoplankton communities (Sommer 1993; Rocap *et al*. 2003; Huisman *et al*. 2004). For instance, the *Prochlorococcus* complex in the oligotrophic ocean is differentiated into several different ecotypes (Moore *et al*. 1998; Rocap *et al*. 2003; Johnson *et al*. 2006). Some of these ecotypes are adapted to high light intensities near the water surface, whereas other ecotypes are adapted to low light intensities encountered at greater depths.

This study builds on previous work of plankton ecologists, who have pointed out that the light spectrum is an important additional axis of niche differentiation (Engelmann 1883; Wood 1985; Kirk 1994), and may play a major selective role in phytoplankton communities (Béjà *et al*. 2001; Rocap *et al*. 2003). Recent laboratory competition experiments demonstrated that partitioning of the light spectrum enables stable coexistence of red and green picocyanobacteria in white light (Stomp *et al*. 2004). Our results show that, essentially, these lab findings can be extrapolated to natural waters. Distribution patterns of picocyanobacteria of the *Synechococcus* complex are strongly related to the underwater light colour, with a gradual transition from predominance of red strains in clear waters to green strains in turbid waters (Fig. 2.5). Moreover, consistent with the model predictions, we found widespread coexistence of red and green picocyanobacteria in many aquatic ecosystems all over the world. This global pattern is consistent with various local studies, which have shown dominance of red picocyanobacteria in the open ocean (Li *et al*. 1983; Platt *et al*. 1983; Campbell & Carpenter 1987; Campbell & Vaulot 1993), and coexistence of red and green picocyanobacteria in waters of intermediate turbidity, such as coastal ecosystems, estuaries and lakes (Pick 1991; Vörös *et al*. 1998; Murrell & Lores 2004; Katano *et al*. 2005; Mózes *et al*. 2006).

Although we focused here on red and green picocyanobacteria, other phytoplankton groups will be involved in competition for light as well. For instance, the absorption spectra of green algae, diatoms, and prochlorophytes all partially overlap with the absorption spectra of red and green picocyanobacteria, and may thereby suppress their numbers. Adding *Prochlorococcus* to our model (results not shown) revealed that, due to their pigmentation in the blue part of the spectrum, *Prochlorococcus* is predicted to dominate competition for light in the clearest oceans. In slightly more turbid waters, *Prochlorococcus* was gradually replaced by red picocyanobacteria, which in turn were gradually replaced by green picocyanobacteria in turbid waters (as in Fig. 2.5). Thus, in principle at least, the theoretical framework presented here can be further extended to define the spectral niches of other phytoplankton groups as well.

A restriction of our competition model is that it assumes complete mixing of the phytoplankton species throughout the surface mixed layer. This may be a reasonable approximation for turbulent surface waters, and demonstrates that vertical stratification is not

required for the coexistence of red and green phytoplankton species. Many waters, however, are not well mixed. Moreover, some cyanobacterial species can regulate their buoyancy, and thereby adjust their vertical position within the water column. An example is *Planktothrix rubescens*, a red filamentous cyanobacterium that can develop dense monolayers in the metalimnion of stratified lakes (Dokulil & Teubner 2000; Walsby 2005). In principle, our phytoplankton competition models can be extended to include weak vertical mixing, using systems of partial differential equations (Klausmeier & Litchman 2001; Huisman *et al.* 2006). It would be an interesting next step to investigate how weak mixing favours species with different pigment composition at different depths.

The analogy between niche differentiation of picocyanobacteria and niche differentiation of Darwin's finches (Darwin 1859; Lack 1974; Grant & Grant 2002) is interesting. Niche differentiation among Darwin's finches has been ascribed to the evolutionary process of adaptive radiation, during which a single ancestor radiated into different species occupying different niches along the spectrum of different seed sizes. Is niche differentiation of picocyanobacteria along the light spectrum the result of a similar process of adaptive radiation? All cyanobacteria contain the bluegreen pigment phycocyanin, whereas only some strains contain the red pigment phycoerythrin. Molecular phylogenies have shown that clusters of closely related picocyanobacteria often contain both red and green strains (Crosbie *et al*. 2003; Ernst *et al*. 2003), as exemplified by the closely related red and green picocyanobacteria from the Baltic Sea (Fig. 2.4c). This may indicate that the ancestral strains of these clusters all contained both phycocyanin and phycoerythrin, or that different clusters acquired red pigments during independent adaptive radiations, by mutation or horizontal gene transfer (Ernst *et al*. 2003). Perhaps evolutionary experiments, similar to ongoing experiments with *E. coli* (Lenski & Travisano 1994), might shed further light on the potential for adaptive radiation in these varicoloured picocyanobacteria.

In conclusion, the theory and field data presented here show that niche differentiation along the underwater light spectrum offers ample opportunities for coexistence of phytoplankton species. These findings add a colourful new solution to Hutchinson's (1961) classic paradox of the plankton, and suggest that the underwater light spectrum deserves full attention in future studies of phytoplankton competition.

Acknowledgements

We thank the crew of the research vessels Aranda and Kilo Moana for help during sampling, D.M. Karl for the opportunity to join HOT cruise 174, and B. Pex, H. van Overzee and R. Poutsma for their help in the Dutch lakes. We also thank A. Wijnholds-Vreman for support with the flow cytometer, H.J. Gons, S.G.H. Simis and P. Stol for help with the filterpad method, and G.G. Mittelbach and the anonymous referees for their helpful comments on the manuscript. M.S. and J.H. were supported by the Earth and Life Sciences Foundation (ALW), which is subsidised by the Netherlands Organization for Scientific Research (NWO). L.V. was supported by the Hungarian Research Fund (OTKA TO-42977). T.H. and L.J.S. acknowledge support from the European Commission through the project MIRACLE (EVK3-CT-2002–00087).

Supplementary Material

The following supplementary material is available for this article:

Table S1 Overview of the 70 sampling stations used in this study.

Appendix S1 Sampling stations.

Appendix S2 Measurement of background turbidity.

Appendix S3 Algorithm to calculate background turbidity.

Figure S1 Light attenuation by phytoplankton versus chlorophyll concentration.

Figure S2 Predicted versus observed background turbidity.

This material is available as part of the online article from: http://www.blackwell-synergy.com/doi/full/10.1111/j.1461-0248.2007.01026.x

Please note: Blackwell Publishing is not responsible for the content or functionality of any supplementary materials supplied by the authors. Any queries (other than missing material) should be directed to the corresponding author for the article.

Table S1 *Sampling stations and some of their characteristics.*

Sampling stations	Area (km^2)	Average depth (m)	Sampling depth (m)	$K_{BG}(484)$ (m^{-1})	Red picos (%)
Hungary, lakes					
L. Balaton (Fűzfő Basin)	596	3.2	0 – 2	1.65	73
L. Balaton (Tihany basin)	596	3.2	0 - 3.7*	2.73	57
L. Balaton (Zánka basin)	596	3.2	0 – 2	1.94	63
L. Balaton (Szigliget basin)	596	3.2	0 – 2	1.49	27
L. Balaton (Keszthely basin)	596	3.2	0 - 2.3*	2.17	73
L. Balaton (Zala river)	-	-	-	3.03	6
Kis-Balaton (upper res.)	18	1	0 – 1*	3.82	0
Kis-Balaton (lower res.)	16	0.8	0 - 0.8*	4.66	0
Marcali reservoir	4	1.8	0 - 1.8*	3.48	0
Monostorapáti reservoir	0.3	2	0 – 2*	6.00	4
L. Pécsi	0.75	3.3	0 - 3.3*	1.41	78
L. Herman Otto	0.29	1	0 – 1*	3.95	32
Deseda reservoir	2.2	2.9	0 - 2.9*	5.90	2
Italy, lakes					
L. Como	146	154	0 – 20*	0.28	98
L. Maggiore	212	177	0 – 20*	0.43	96
L. Garda	368	133	0 – 20*	0.22	98
L. Iseo	62	123	0 – 20*	0.29	99
L. Orta	18	72	0 – 20*	0.46	100
L. Mergozzo	1.8	45	0 – 20*	0.25	99
L. Varese	15	11	0 – 11*	0.69	54
L. Candia	1.3	5.9	0 - 5.9*	0.49	50
L. Paione Superiore	0.014	5.1	0 - 5.1*	0.35	100
L. Paione Inferiore	0.014	7.3	0 - 7.3*	0.12	100
L. Azzuro	0.003	2	0 – 2*	0.30	100
L. Devero	1	20	0 – 20*	0.35	100
Nepal, lakes					
L. Piramide Superiore	0.6	8.2	0 - 8.2*	0.21	100
L. Piramide Inferiore	1.7	14.8	0 - 14.8*	0.12	100
New Zealand, lakes					
Okareka	3.5	12	2	0.30	55
Tarawera	41	50	2	0.36	100
Rotorua	80	6.8	2	0.80	60
Ontario, lakes					
Superior	81900	145	2	0.19	100
Erie (east)	6150	27	2	0.42	100
Erie (central)	15390	18	2	0.32	100
Erie (west)	3680	7.6	2	0.94	67

Sampling stations	Area (km^2)	Average depth (m)	Sampling depth (m)	$K_{BG}(484)$ (m^{-1})	Red picos (%)
Ontario	19680	90	2	0.41	100
Bay of Quinte	257	8.3	2	2.15	11
Cherry	0.22	5.5	2	0.83	16
Triangle	0.27	4.7	2	0.59	49
Bay	1.6	11	2	0.35	100
Buller	0.31	20	2	0.46	100
Halls	5.7	?	2	0.24	88
Koshlong	4.1	10	2	0.48	68
Anstruther	6.3	13	2	0.69	19
L'Amable	1.8	23	2	0.48	100
Opeongo	22	?	2	1.21	21
St. Nora	?	?	2	0.91	52
Crawford	0.02	?	2	0.45	100
Drag	10	18	2	0.48	92
Wolf	1.2	4.8	2	0.86	35
Picard	0.76	10	2	0.48	99
Salmon	1.7	11	2	0.35	100
Bobs GB	4.8	14	2	0.41	93
Chub	0.34	8.8	2	0.85	0
Jacks	5.1	17	2	0.57	95
Bobs WB	9.4	9.5	2	0.74	66
St. George	0.10	/	2	0.66	53
Rice	100	2.4	2	1.52	18
Heart	0.18	3.7	2	2.34	0
Alberta, lakes					
Island	7.8	3.7	2	0.76	90
Amisk	5.2	16	2	1.11	91
Baltic Sea					
LL3A	3.7×10^5	69	0 – 20*	0.86	55
CYA04_2	3.7×10^5	75	0 – 14*	0.31	77
CYA04_3	3.7×10^5	63	0 – 17*	0.70	69
CYA04_7	3.7×10^5	85	0 – 14*	0.63	72
CYA04_11	3.7×10^5	77	0 – 15*	1.17	39
CYA04_15	3.7×10^5	69	0 – 15*	0.67	66
CYA04_20	3.7×10^5	62	0 – 30*	0.56	51
CYA04_22	3.7×10^5	90	0 – 20*	0.71	52
CYA04_28	3.7×10^5	111	0 – 40*	0.52	65
Pacific Ocean, Hawaii					
ALOHA	N.A.	~4000	0 – 120*	0.016	100

**Samples were integrated over the depth of the surface mixed layer*

Appendix S1

Sampling stations

During the summers of 1986-1988, 30 lakes in Canada and 3 lakes in New Zealand were sampled, covering a wide range in background turbidities and water-column depths (Pick 1991). For each lake, 8-12 samples were taken from 2 m depth using a Van Dorn sampler. These samples were mixed.

During the summers of 1994 and 1995, 13 lakes in Hungary, 12 lakes in Italy and 2 lakes in Nepal were sampled (Vörös *et al*. 1998). In the deep lakes, the first 20 m of the water column was sampled with an integrating sampler. In the shallow lakes, ponds and reservoirs the whole water column was sampled by a Van Dorn sampler using an interval of 1 m, and these samples were mixed.

From 12 to 19 July 2004, 9 stations in the Baltic Sea (from 59.1°N to 60.0°N and from 22.2°E to 26.2°E) were sampled from the research vessel Aranda on Cruise Cyano-04 08/2004. Water samples were taken with a Rosette sampler from 0 to 30 m depth using a sample interval of 3 m. Temperature was measured using the Seabird 911 plus CTD sonde.

From 5 to 11 October 2005, Station ALOHA (23.4°N, 158°W) of the Hawaiian Ocean Time series (HOT) in the North Subtropical Pacific Ocean was sampled from the research vessel Kilo Moana on cruise number 174. Water samples were taken from 12 depths within the upper 200 m with a SeaBird (Model SBE-09) CTD Rosette system. An overview of all 70 sampling stations is given in Table S1.

Appendix S2

Measurement of background turbidity

To calculate the underwater light field, the model uses the background turbidity at the reference wavelength of 484 nm, $K_{BG}(484)$, as input parameter (Eq.4 of the main text). We determined $K_{BG}(484)$ spectrophotometrically, as the sum of the light absorption by gilvin, $K_{GIL}(484)$, and the light absorption by tripton, $K_{TRIP}(484)$.

Absorption by gilvin

Dissolved organic matter is known as 'gilvin' in the optics literature. To determine light absorption by gilvin, water samples were filtered through 0.2 μm cellulose acetate filters (Schleicher and Schuell). Absorption spectra of the filtrate were measured by a Lambda 800 UV/VIS spectrophotometer (Perkin-Elmer, Wellesley, MA, USA) using a 5 cm quartz cuvet, with milli-Q water as reference (Simis *et al*. 2005). The parameter $K_{GIL}(484)$ is the light absorption by gilvin measured at 484 nm.

Absorption by tripton

Tripton refers to inanimate suspended particles in the water column. Absorption spectra of suspended matter were determined on GF/F filters using the filterpad method (Yentsch 1962; Cleveland & Weidemann 1993; Simis *et al*. 2005). The spectra were measured with a Lambda 800 UV/VIS spectrophotometer (Perkin-Elmer, Wellesley, MA, USA) equipped with a 150-mm integrating sphere (Labsphere, North Sotton, NH, USA). For the correction of path length amplification the method of Cleveland and Weidemann (1993) was used. First, the absorption spectrum of the loaded filter, obtained after filtration of the water sample, was measured. This includes all seston (phytoplankton plus tripton). As a next step, the absorption spectrum of tripton on the filter was measured, after bleaching of phytoplankton pigments by boiling ethanol. The parameter $K_{TRIP}(484)$ is the light absorption by tripton measured at 484 nm.

Appendix S3

An algorithm to calculate background turbidity

Ideally, one would like to determine the background turbidity from direct measurements of the light absorption by gilvin and tripton, as described in **Appendix S2**. However, for several sampling stations we did not have data on the absorption by gilvin and tripton. Therefore, we developed a simple algorithm to calculate the background turbidity from the total light attenuation coefficient and the chlorophyll concentration in the water column. This Appendix presents a concise description of the algorithm.

Partitioning of the total light attenuation

The total light attenuation, K_D, in natural waters is governed by light attenuation by gilvin and tripton, K_{BG}, attenuation by water itself, K_W, and attenuation by phytoplankton, K_{PHYT} (Kirk 1994). Hence, the total light attenuation at the reference wavelength of 484 nm can be partitioned as follows:

$$K_D(484) = K_{BG}(484) + KW(484) + K_{PHYT}(484) \qquad \text{(S1)}$$

Accordingly, $K_{BG}(484)$ can be calculated if the values of the other attenuation coefficients in Eq S1 are known. The total light attenuation coefficient at 484 nm, $K_D(484)$, was estimated

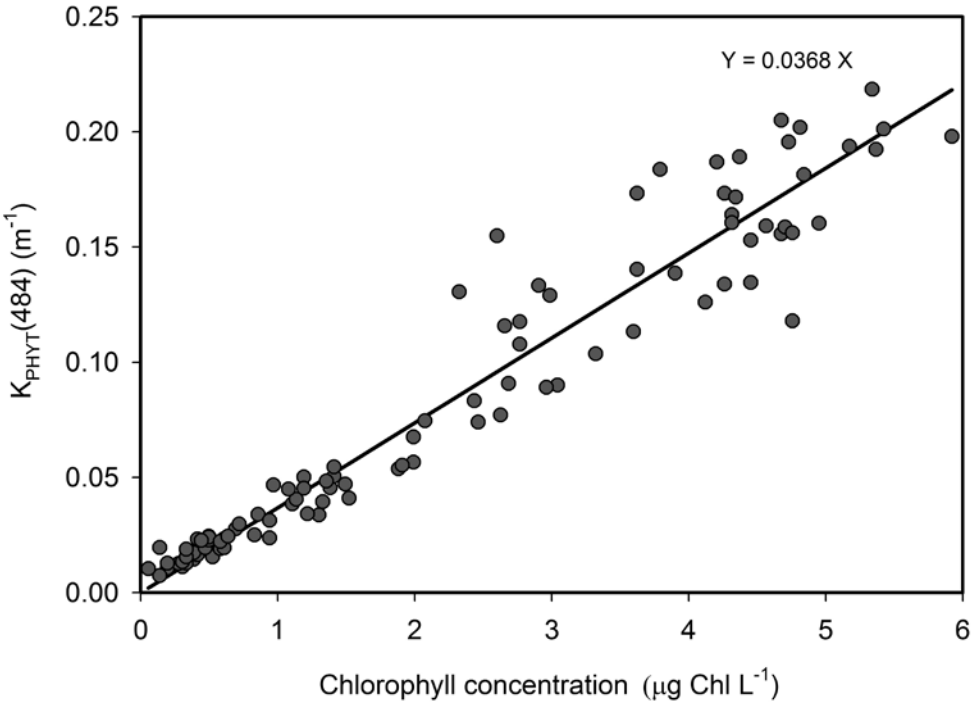

Figure S1 *Light attenuation coefficient of phytoplankton at 484 nm, $K_{PHYT}(484)$, as function of the chlorophyll a concentration.*

from the attenuation coefficient of photosynthetic active radiation, K_D(PAR), using the empirical relation (Balogh *et al*. 2000):

$$^{10}log\,[K_D(484)] = 1.1353\,^{10}log\,[K_D(PAR)] + 0.2023 \qquad \text{(S2)}$$

where K_D(PAR) was estimated from vertical light profiles (PAR range, 400-700 nm), measured with a Licor Li-185 quantum sensor for the Baltic Sea and the lakes in Hungary, Italy and Nepal and with a Licor Li-190 quantum sensor for the lakes in Canada and New Zealand. Light attenuation by pure water at 484 nm is known, i.e., K_W(484) = 0.0136 m^{-1} (Pope & Fry 1997). Light attenuation by phytoplankton, K_{PHYT}(484), was calculated from chlorophyll *a* concentrations, as described below.

Absorption by phytoplankton at 484 nm

We established a relationship between K_{PHYT}(484) and the chlorophyll concentration. For this purpose, samples from 10 sampling stations in the Baltic Sea, at 11 different depths per sampling station, were each split into two subsamples. One set of subsamples was used for chlorophyll analysis while the other set of subsamples was used to determine the phytoplankton absorption spectra. Chlorophyll *a* concentrations were measured spectrophotometrically after hot ethanol extraction of phytoplankton collected on Whatman GF/F filters (Nusch 1980).

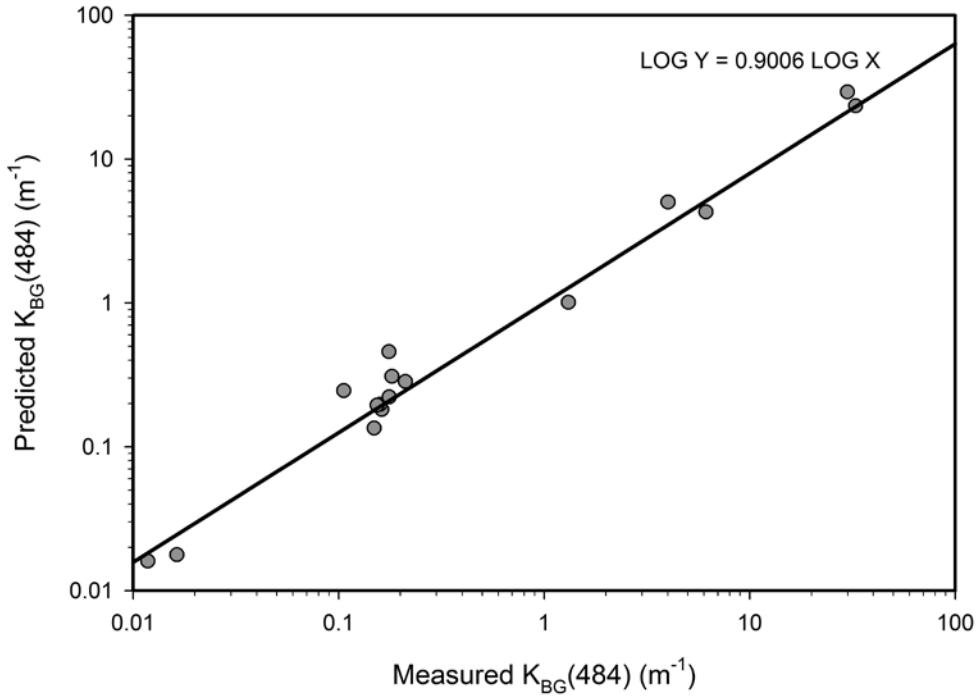

Figure S2 *Background turbidity predicted from Eqs S1-S3 against measured background turbidity. Data points represent samples taken from five Dutch lakes (Lake Loosdrecht, Lake Proost, Lake Groote Moost, Lake t'Elfde, Lake IJsselmeer), nine sampling stations in the Baltic Sea, and two sampling stations near station ALOHA (Pacific Ocean, Hawaii).*

Light absorption spectra of the phytoplankton communities were obtained from the filterpad method described in **Appendix S2**, as the difference between the absorption spectrum of seston (phytoplankton plus tripton) and the absorption spectrum of tripton. The results show a strong relationship between the phytoplankton light absorption at 484 nm and the chlorophyll *a* concentration (Fig. S1):

$$K_{PHYT}(484) = 0.0368\,[Chl] \qquad \text{(S3)}$$

where [Chl] is the chlorophyll *a* concentration in μg Chl L^{-1} (linear regression forced through the origin: $R^2 = 0.93$, n=110, $p<0.0001$). Eq. S3 was used to calculate $K_{PHYT}(484)$ from the chlorophyll *a* concentrations for all sampling stations.

Calibration of the algorithm

The background turbidity, $K_{BG}(484)$, can now be calculated from Eqs S1-S3. To test this, we compared the predicted background turbidity (Eqs.S1-S3) with the measured background turbidity (Appendix S2). For this purpose, we applied Eqs S1-S3 to an independent data set consisting of five Dutch lakes (Lake Loosdrecht, Lake Proost, Lake Groote Moost, Lake t'Elfde, Lake IJsselmeer), nine sampling stations in the Baltic Sea, and two stations near station ALOHA (Pacific Ocean, Hawaii), and at these sites we also measured the background turbidity following the procedures described in Appendix S2.

This showed a close correspondence between the predicted and measured background turbidity (Fig. S2):

$$^{10}log\,[K_{BG,pred}(484)] = 0.9006\,^{10}log\,[K_{BG,meas}(484)] \qquad \text{(S4)}$$

based on linear regression forced through the origin, after log-transformation of the data (R^2= 0.98, n=16, $p<0.0001$). The factor 0.9006 in Eq.S4 was incorporated as correction factor in the algorithm to improve our predictions.

Hence, combining the information in Eqs S1-S4, the following algorithm was obtained to predict the background turbidity at 484 nm from the light attenuation coefficient and chlorophyll *a* concentration:

$$K_{BG}(484) = \left[1.593\,[K_D(PAR)]^{1.135} - 0.0136 - 0.0368\,[Chl]\right]^{1.11} \qquad \text{(S5)}$$

We applied this semi-empirical algorithm to calculate the background turbidity at all 71 sampling stations. Furthermore, we suggest that the algorithm may also find application in other studies.

Supplementary References

Balogh, K.V., Koncz, E. & Vörös, L. (2000). An empirical model describing the contribution of colour, algae and particles to the light climate of shallow lakes. *Verh. Internat. Verein. Limnol.*, 27, 2678-2681.

Cleveland, J.S. & Weidemann, A.D. (1993). Quantifying absorption by aquatic particles: a multiple scattering correction for glass-fiber filters. *Limnol. Oceanogr.*, 38, 1321-1327.

Kirk, J.T.O. (1994). *Light and Photosynthesis in Aquatic Ecosystems* (2nd edn). Cambridge Univ. Press, Cambridge.

Nusch, E.A. (1980). Comparison of different methods for chlorophyll and phaeopigment determination. *Arch. Hydrobiol. Beih. Ergebn. Limnol.*, 14, 14-36.

Pope, R.M. & Fry, E.S. (1997). Absorption spectrum (380-700 nm) of pure water. II. Integrating cavity measurements. *Appl. Opt.,* 36, 8710-8723.

Pick, F.R. (1991). The abundance and composition of freshwater picocyanobacteria in relation to light penetration. *Limnol. Oceanogr.*, 36, 1457-1462.

Simis, S.G.H., Peters, S.W.M. & Gons, H.J. (2005). Remote sensing of the cyanobacterial pigment phycocyanin in turbid inland water. *Limnol. Oceanogr.*, 50, 237-245.

Vörös, L., Callieri, C., Balogh, K.V. & Bertoni, R. (1998). Freshwater picocyanobacteria along a trophic gradient and light quality range. *Hydrobiologia,* 370, 117-125.

Yentsch, C.S. (1962). Measurement of visible light absorption by particulate matter in the ocean. *Limnol. Oceanogr.*, 7, 207-217.